

Interactive comment on “The hydraulic efficiency of single fractures: Correcting the cubic law parameterization for self-affine surface roughness and fracture closure” by Maximilian O. Kottwitz et al.

Maximilian O. Kottwitz et al.

mkottwi@uni-mainz.de

Received and published: 8 April 2020

We sincerely thank Guido Blöcher for his review. His comments were very useful and helped us to improve the quality of our manuscript. Please find below a point-by-point response to the general and specific comments (comments of the reviewer in black and our response in red, text changes appear in italic font) .

On behalf of all authors, Yours sincerely,

C1

Maximilian Oskar Kottwitz

General comments:

The general focus of the paper is to present a correction factor for the cubic law in the R-S space. This by its own is of particular interest. In contrast, all simulations were performed with a pressure difference of 0.01 Pa and laminar flow conditions are assumed. This opens the question, are the correction factors the same (in R-S space) for other pressure gradients and therefore other flow velocities.

Laminar flow conditions are essential for using the Stokes equations instead of the Navier-Stokes equations and are valid for Reynolds numbers below unity (see Zimmermann & Bodvarsson, 1996). Above that, inertial forces start to introduce turbulences which further reduce overall flowrates. By choosing a constant pressure difference of 0.01 Pa, we ensured that the maximal resulting Reynolds numbers is below unity. In figure 1, we show the Reynolds number Re (computed by $Re = \frac{\rho \bar{v} \bar{a}}{\mu}$, with fluid density ρ , volume average velocity \bar{v} , mean aperture \bar{a} and fluid viscosity μ) as function of mean aperture \bar{a} . As evident from the picture, the bulk of the simulations range from 10-3 to 10-8. Which means, for sub-millimeter apertures, the pressure gradient could be larger than 0.01 Pa without interfering with the unity threshold. For sub-centimeter apertures, we reach the unity threshold, so strictly speaking, this poses an upper limit for the applicability of the computed correction factors. For pressure differences lower than 0.01 Pa, we generally assume the correction factors to be valid. If fractures with larger apertures (e.g. cm range) are considered, the applied pressure gradients need to be reduced such that they fulfill the above-mentioned criteria of Reynolds numbers

C2

below unity. Yet, if laminar flow conditions exist, the proposed correction factors remain applicable.

Although, a non-dimensional fracture roughness quantification-scheme is acquired, the authors could indicate the dimensions of their simulations. This would help to understand at which scale the correction scheme is applicable. Values of length, height, mean aperture, etc. should be mentioned either as absolute or relative values.

We indicated a fixed physical voxel size of 0.1 mm. With a constant model resolution of 512*512*128 voxels, this results in a model size of 51.2*51.2*12.8 mm. Table 1 gives input metrics used to generate the synthetic fractures. The resulting range of mean apertures ($\bar{a}_{min} = 1.910 * 10^{-4}$ m; $\bar{a}_{max} = 4.961 * 10^{-3}$ m) as well as absolute permeability values ($k_{min} = 6.786 * 10^{-14}$ m²; $k_{max} = 7.940 * 10^{-7}$ m²) were inserted a new table (table 2) at page 9.

This comment is the most important one. As mentioned before the presented approach seems highly applicable. Unfortunately, the proof with real data is missing. It would be nice to use, e.g. laboratory measurements, to proof the presented approach. If no data are available, we could provide surface scans with a resolution of 50 μ m and related fracture permeability measurements. Furthermore, aperture distribution, mean aperture, contact area are known. The authors could show how they determine the S-R-values and can subsequently compare the corrected permeability values with the measurements. (contact: Guido Blöcher, bloech@gfz-potsdam.de)

The validation of the proposed concept with real data is truly of high interest. In fact, we are already preparing follow-up studies targeting exactly this:

In one study, we validate the results of the numerical simulations by using 3D printed

C3

versions of some fracture realizations generated in this study and perform laboratory experiments to obtain their permeabilities to subsequently compare them to their numerical equivalents.

In another study, we test the performance of the proposed correction scheme to predict permeabilities of real fractures by utilizing CT-scans of those (partly obtained from www.digitalrockspotal.org and partly self-acquired – by now a total of 32 CT-scans). It also incorporates simple pre-processing advices to prepare the CT data for numerical simulations and the computation of the S-R-values, which we by default calculate from voxel datasets.

We genuinely appreciate the offer of providing data, especially the fracture permeability measurements are of high interest. However, to fully capture the statistics of a fracture's aperture field (specifically in terms of its correlation length and contact areas) we require volumetric (voxel-based) data, rather than separated scans of fracture surfaces. By that, we hope to reflect the true matching of the opposing fracture surfaces, which determines the correlation length of the aperture field. Furthermore, we computed the S-R-values from volumetric data.

We fully understand the request for a proof with real data, however we think that this is beyond the scope of this methodological study and we think that it is more appropriate to deliver this in future studies.

Specific comments:

P1L2: Replace "Yet" with "In contrast".

Incorporated suggest change at indicated location.

C4

P1L9: Here a sentence regarding the dimension of the simulation (length, width, and aperture) should be added.

We changed the sentence at P1L10 to:

Each fracture consists of two random, 25cm² wide self-affine surfaces with prescribed roughness amplitude, scaling exponent, and correlation length, which are separated by varying distances (mean apertures in submillimeter range) to form fracture configurations that are broadly spread in the newly formed two-parameter space.

P3L75: What means: low Reynolds numbers and low-pressure gradients? The authors should provide ranges where the presented approach is applicable.

We changed the sentence at P3L75 to:

Assuming, that the flow is solely laminar (Reynolds numbers below unity according to Zimmermann and Bodvarsson, 1996), the fluid viscosity is constant and ...

P3L81: What is effective fluid viscosity? μ is the dynamic fluid viscosity.

We simplified the sentence at p3L81 to:

... with the fluid's dynamics viscosity μ , ...

Figure 2: The vertical axis has no axis label. It seems it indicates the aperture. Since the aperture is provided by the color code, a 2D image would be sufficient.

Technically, a 2D image would be sufficient as vertical axis and colorbar provide the same information. However, we choose the 3D representation to put emphasis

C5

on the effective surface area increase caused by a lower Hurst exponent for equal mean and standard deviations. In 2D, we had the impression that this was not as straightforward to see. On top of that, the necessary visual comparison of mean and standard deviation by the black solid and dashed lines could not be realized in 2D.

This is why we would rather keep the Figure as is, while changing the caption as follows:

Two aperture fields constructed from synthetic fractures. Both aperture fields are based on the same sets of random numbers with varying Hurst exponents H, which is a) 0.4 and b) 0.8. The two statistical parameters \bar{a} and σ_a are indicated by black solid and dashed lines, respectively. Axis units are in mm, while the vertical axis (indicating aperture) is exaggerated by a factor of two for clarity. Note that \bar{a} and σ_a are identical for a) and b). Increasing height fluctuations at smaller scales, caused by a lower Hurst exponent results in a larger effective surface area S for fracture a) compared to b).

P6L126: Often ϕ indicates the porosity but not here. I suggest using another symbol than ϕ to indicate the correction factor.

We decided to change the symbol from ϕ to χ throughout the paper, as we agree that the use of ϕ can lead to confusion.

P6L128: For $S = 1$ and $R = 0$ we would mimic flow between parallel plates. For this situation, the correction factor should be one and the cubic law could validate the simulation. This validation was done but is somehow hidden in figure 5. The authors should emphasize that this simple check was performed.

We added the following sentence at P9L197:

Perfect hydraulic efficiencies ($\chi = 1$) were validated by flow simulations in parallel-plate

C6

fractures.

P6L135: Why a representation of the matrix is required? Only the fracture is simulated and the boundary condition is a non-slipping boundary. It is not clear why the complete matrix-fracture-system is considered.

Numerically, we don't discretize the matrix. We zero out the corresponding entries in the jacobian matrix to gain computation time. However, we ensure constant spatial extents for all simulations for the volume integration of the velocity, such that all permeabilities are normalized to the same fracture volume.

P6L136-138: The sentence seems to be incomplete and should be rewritten. Furthermore, the macroscopic flow direction (y-direction) should be mentioned.

We changed the sentence at P6L136-138 to:

Different pressures are applied on two opposing boundaries ($\Delta P = 0.01 \text{ Pa}$ for all models), while the remaining boundaries are set to no-slip. This fixes the principal direction of fluid movement (here it is in y-direction, e.g. Fig. 3).

P6L141: This is an integration of v_y over the total volume and not a volume integral. Since v_x and v_z should be small compared to v_y these quantities could be used to determine $v \parallel E$.

For directional permeabilities, we are just interested in the v_y component for the applied boundary conditions (no-slip at boundaries next to pressure boundaries). Considering of v_x and v_z would only be important, if we open the no-slip boundaries

C7

(e.g. apply a linear gradient between opposing fracture boundaries).

We updated the sentence at P6L141:

After ensuring that the numerically converged solution is obtained (see appendix A in Eichheimer et al., 2019), the velocity component parallel to the principal flow direction is integrated over the volume to compute the volume average velocity \bar{v} according to:

...

P6L144: The dynamic viscosity is denoted with η before it was μ .

We changed the viscosity notation to μ .

Table 1: The number of parameter combinations for group 1 is given to be 400. If I multiply the n_{g1} ($4^*4^*4^*5$) it should be 360. Furthermore, the fracture configurations for group 1 should be $360^*r_{g1}=7200$ but only 6400 are mentioned in the table caption.

Apologies, we indeed forgot to update the total number of parameter combinations to 320 ($4^*4^*4^*5$). This results in 6400 geometries and 12800 flow simulations.

P8L157: Again, values about the fracture aperture and the representation by the voxels is missing.

We expanded the sentence at P8L157 by:

... with a fixed physical voxel size of 0.1 mm, resulting in a model domain of 51.2 x 51.2 x 12.8 mm.

We added the following at P8L166:

C8

..., yet they all remain fully percolating (resulting mean apertures range from 0.15 to 4.96 mm).

P8L173: 12800 flow simulations are mentioned assuming 6400 fracture configurations. If comment 12 is corrected or explained the authors should revise the number of flow simulations (14400).

See comment above.

P9L194: In case the authors decided for another symbol than ϕ , they should correct the symbol here.

See comment above. Symbol was also changed in Figure 5 and Figure 7.

Figure 5: The figure is fine in color mode but almost no difference between blue and red is visible in greyscale mode. Maybe, the color scheme can be adjusted.

We revised the figure with a grey-scale friendly and also sequential colorbar (see figure 2), which makes more sense than a diverging one. Colour descriptions in the figure caption are changed accordingly.

P13L240: Please add a space after closure.

We incorporated suggest change at indicated location.

C9

Figure9: The mean error norm was obtained for the considered fractures and applied boundary conditions. The authors should discuss if this error norm changes for other flow regimes regarding Reynold number, flow velocity, pressure gradients, etc..

Increasing the pressure gradient results in higher flow velocities, ultimately leading to larger Reynolds numbers. As discussed above, the results are only valid, if the Reynolds number is below or equal to unity, i.e. laminar flow conditions are present, which is a fundamental assumption of using the Stokes equations. Quantifying errors in flow regimes other than laminar would require solving the full Navier-Stokes equations, which is beyond the scope of this study but poses an interesting challenge for future work.

Interactive comment on Solid Earth Discuss., <https://doi.org/10.5194/se-2019-190>, 2020.

C10

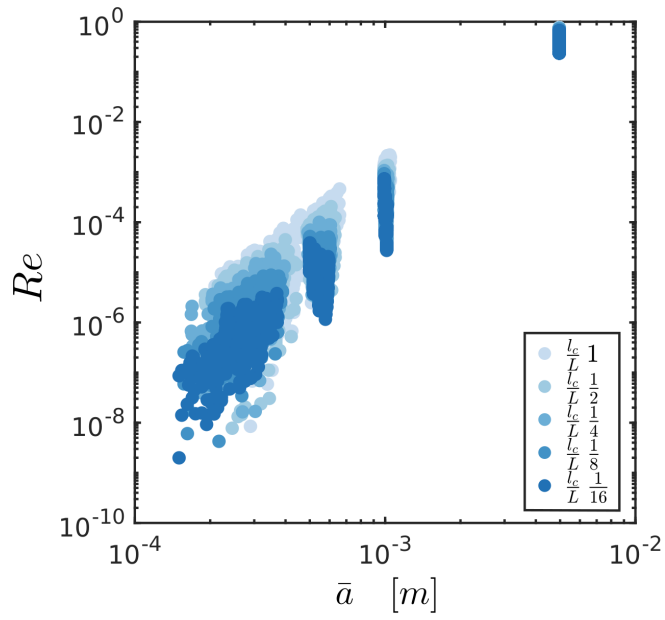


Fig. 1. Computed Reynolds number as function of mean aperture for different correlation-length-to-size ratios

C11

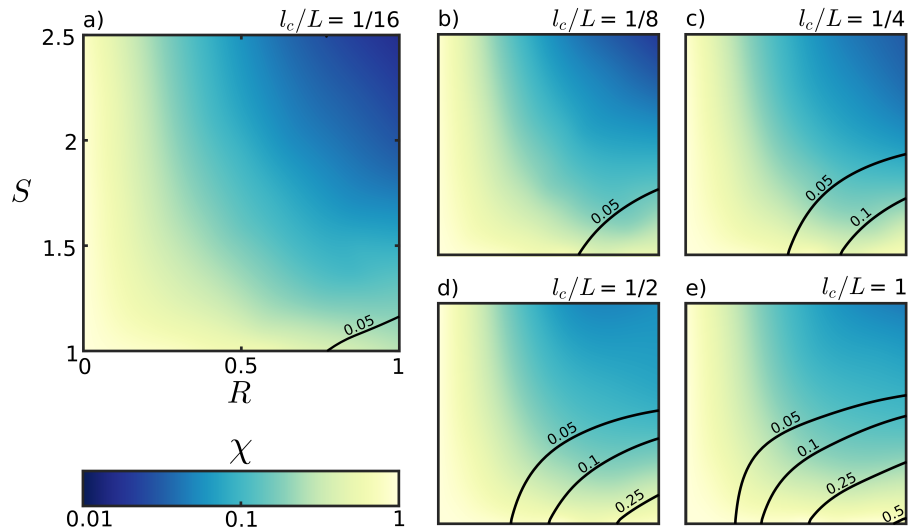


Fig. 2. The distribution of the hydraulic efficiency for different correlation-length-to-size ratios as function of R and S

C12